行政院國家科學委員會專題研究計畫 成果報告

以無機分子改質雙性機丁聚糖之自組裝混成複合材料及其生醫特性之研究

研究成果報告(精簡版)

計 畫 類 別 ：個別型
計 畫 編 號 ：NSC 98-2113-M-009-004-
執 行 期 間 ：98 年 08 月 01 日至 99 年 07 月 31 日
執 行 單 位 ：國立交通大學材料科學與工程學系（所）

計 畫 主 持 人：劉典謨

計畫參與人員：碩士班研究生-兼任助理人員：董簪華
碩士班研究生-兼任助理人員：劉佩鈴

處 理 方 式 ：本計畫可公開查詢

中 華 民 國 99 年 09 月 23 日

期末報告

計畫編號:NSC 98-2113-M-009-004

計畫名稱:

以無機分子改質兩性幾丁聚醣之自組裝混成複合材料及其生醫特性之研究

執行機構: 國立交通大學材料科學與工程學系

主持人: 劉典謨 副教授

09-17-2010

摘要

藉由兩性幾丁聚醣(縮酸基改質親水端，長碳鏈改質疏水端)與矽烷基偶聯劑 APTES，(3-Aminopropyl) triethoxysilane，以化學鍵結方式結合，成功地合成出一無機-有機混成分子，並同時具有在水溶液中自組裝的功能。我們經由 FTIR 與 ^{13}C-, ^{29}Si 固態核磁共振儀鑑定此無機-有機混成分子之化學結構; 而在水溶液中自組裝行為則由臨界微胞濃度(Critical aggregation concentration)來觀察，發現其自組裝的行為與分子在水溶液中的濃度有關。其自組裝形成的奈米載體之外觀形貌由掃描式電子顯微鏡(scanning electron microscopy, SEM)與穿透式電子顯微鏡(transmission electron microscopy, TEM)來觀察，其粒徑大小則由 DLS 偵測。此有機-無機混成分子在水溶液環境中自組裝所形成的奈米微粒，由穿透式電子顯微鏡的影像，可觀察到層狀二氧化矽的結晶相，推測在此有機-無機混成分子所形成之奈米微粒，無機二氧化矽是以 shell 或 layer-by-layer 的形式存在，此二氧化矽 layer 是以連續且高度整齊排列成 4~6 奈米之間的原子層，推測此連續且高度整齊排列二氧化矽的產生，與此混成分子在水溶液中自組裝的行為所導致有關，疏水的作用力誘引此混成分子中之原子自我組織成一整齊的排列方式。二氧化矽層在此混成奈米微粒中，扮演著物理屏障的角色，可以減少包覆之內容物隨著高分子在水溶液中膨潤現象的產生而擴散溢出。此二氧化矽層的存在，顯示了一潛在的新可能性。

1. Introduction

1-1 Introduction

In recent years, development of advanced organic-inorganic hybrids has become one of the most innovative research fields. The synthesized materials, which combine organic macromolecules with inorganic components, allow the properties tunable from atomic, mesoscopic, to macroscopic scale and also successfully integrated the advantages of both organic and inorganic materials to meet various industrial demands. The ability to manipulate outstanding chemical, physical, and biological properties from individual, i.e., organic and inorganic, component provides opportunities to expand wider applicability in various fields, from catalysis, optics application, to biomedical devices, etc. [1-3,18] Many approaches for the preparation of hybrid compounds were recently reported. Among them, the synthesis of composite through the combination of polysaccharides and silicon-based materials has been widely reported in various fields, such as enzyme immobilization, porous materials and electrochemical sensors [1-7]. Furthermore, chitosan-based materials have been proposed for a range of biomedical applications [1-4, 26]. Among those relevant reports, chitosan-based hybrid molecules capable of self assembling into well-organized architecture have been rarely found. It is currently an important research objective by integrating diverse functions into a given nanoobject for advanced applications. This is particularly interesting in the area of biomedical and pharmaceutical industries.

Taking the advantage of outstanding biocompatibility of natural polymers, such as chitosan or its modified analogs, associated with unique functions of inorganic component, it is highly potential to design a new hybrid molecule that imparts technically desirable behavior for biomedical demands. The use of pristine chitosan or its composite analogs has been widely reported for drug delivery practice. However, for most polymeric drug delivery nanoparticles reported in literature, burst-like elution of drug has frequently observed in the early-phase delivery in-vitro and in-vivo, which is mainly due to swelling effect of the polymer. This effect turns to be more pronounced for those water-soluble polymers or most of natural polymers. Adsorption of drug near the surface region of a nanocarrier upon drug encapsulation may cause uncontrollable loss or leakage upon delivery, making a final therapeutic dose less efficacy. Moreover, many water-soluble natural polymers exert less preference to encapsulate water-insoluble drugs, albeit some emulsification technologies or analogous skills have been developed to compromise the deficiency. Therefore, to minimize those undesirable effects and in the meantime, impart improved medical or pharmaceutical potential to a new nanocarrier, it is more desirable to employ and modify a natural macromolecule that is able to undergo self assembly to effectively entrap water-insoluble drug for a subsequent control drug elution.

Here we report a novel hybrid molecule through the employing of an amphiphilic chitosan which was successfully synthesized from this lab, as a model macromolecule. Following a

previous work on the synthesis of this amphiphilic chitosan [8], where the amino groups, -NH_2, of the carboxymethyl chitosan chain were replaced partially by hydrophobic hexanoyl group, a further chemical modification along the chain was performed using a coupling agent, (3-aminopropyl)triethoxysilane (APTES). In this study, we successfully synthesized a new hybrid macromolecule which was prepared through the chemical bonding between the amphiphilic chitosan and APTES precursor. The nanostructure, physical and biological properties, and drug encapsulation/release behavior of the novel hybrid molecule were systematically investigated.

1-2 Literature Review

1-2-1 Introduction of Particulate Carriers Based on Chitosan

chitosan (CS), β-(1,4)-link glucosamine unit, is produced by deacetylation of chitin, which is extracted from the shells of crabs, shrimp, and krill. It exhibits several characteristics such as biocompatibility, nontoxicity, and bioadhesivity which make it as an ideal material for biomedical uses, such as drug delivery [30]. However, its poor solubility in water and common organic solvents has so far limited its wide-spread utilization. The reactive amino groups in the backbone of chitosan make it possible to chemically conjugate with various biological molecules [31]. As a result, there have been many works about the methods to enhance the solubility of chitosan, one of which was derivatization. For example, the introduction of

carboxyl groups to chitosan derivatives led to the anionic or amphotheric properties, are water-soluble, and are attracting much attention as metal collecting materials and biomaterials [32]. Hence, hydrophilically, hydrophobically, and amphiphilically modified chitosan derivatives are being studied to form the monodisperse self-aggregated nanoparticles by sonication in aqueous media due to noncovalent association arising from intra- or/and intermolecular interactions among hydrophobic segments in aqueous media [20, 34-35].

During the past decade there has been a growing interest in the investigation of polymeric micelles as a potential carrier for drug delivery. It is well known that polymeric micelles have unique core–shell architecture composing hydrophobic segments as internal core and hydrophilic segments as surrounding corona in aqueous medium. The hydrophobic core provides a loading space for poorly water-soluble drugs. The hydrophilic shell allows polymeric micelle gain the stability in aqueous environment, and the active targeting to tumor cells by further ligand modification [36-38]. Comparing with traditional micelles of low-molecular weight surfactant, polymeric micelles are generally more stable with a relatively lower CMC, and show slower dissociation in aqueous environment [39]. Besides, polymeric micelles own many characteristics as the drug carrier [40]: (1) nano-order size: the micelles can be sterilized by simple filtration, and avoided

mechanical clearance by filtration or in the spleen. (2) Long circulation: it is hard to be recognized and internalized by reticuloendothelial system (RES) because of its hydrophilic

and willowy shell. (3) Solubilization: solubilization of hydrophobic drug is a difficult problem for the clinical application. Fortunately, micellar core can store the insolvable drugs to increase its solubility.

The polymeric micelles as drug carriers based on chitosan were wide-spread researched due to the many advantages of chitosan. The linoleic acid (LA)-grafted chitosan oligosaccharide was synthesized in the presence of 1-ethyl-3-(3-dimethylaminopropyl)carbodiimide (EDC), The results showed that these chitosan derivatives were able to self assemble and form spherical shape polymeric micelles with the size range of 150.7–213.9nm and the zeta potential range of 57.9–79.9 mV, depending on molecular weight of CSO and the charged amount of LA. Using doxorubicin (DOX) as a model drug, The drug encapsulation efficiencies (EE) of DOX-loaded CSO-LA micelles were as high as about 75%, and the drug loading (DL) capacity could reach up to 15%.

Liu L. [19] have prepared chitosan-based copolymers with binary grafts of hydrophobic polycaprolactone and hydrophilic poly(ethylene glycol) (CS-g-PCL&PEG) by a homogeneous coupling reaction of phthaloyl- protected chitosan with functional PCL-COOH and PEG-COOH, following deprotection to regenerate free amino groups back to chitosan backbone. They were characterized by 1H NMR, Fourier transform infrared and X-ray diffraction analysis. These CS-g-PCL&PEG copolymers could form nano-size self-aggregates in acidic aqueous solution without a specific processing technique, which were investigated

using dynamic light scattering and transmission electron microscopy. The formed self-aggregates become smaller with weakened stability upon pH increasing. Moreover, the aggregates of copolymer with higher content of PEG and PCL grafts could remain stable for over 30 days in both acid and neutral condition. A possible mechanism was proposed for the formation of self-aggregates from CS-g-PCL&PEG and their structural changes as pH. It is warranted to find promising application of these self-aggregates based on chitosan as drug carriers.

In our laboratory, a new type of chitosan hollow structure, i.e., carboxymethyl-hexanoyl chitosan (CHC), which was modified first by hydrophilic carboxymethylation to increase the flexibility of chitosan molecular chains in water[33] followed by hydrophobic modification with hexanoyl groups to add amphiphilic character, was employed to study its self-aggregation behavior to form nanocapsule in aqueous solution and nanostructural evolution. The stability of nancapsules and formation mechanism of the CHC macromolecules were explored through the use of critical aggregation concentration (cac), zeta potential, electron microscopy, and dynamic light scatter (DLS). By taking the advantage of self-aggregation nature, the CHC was employed to encapsulate doxorubicin (DOX), an anticancer agent of broad spectrum with reasonable therapeutic index and intriguing biological and physicochemical actions,[41] to further understand its loading efficiency and release behavior.

1-2-2 Inorganic-Organic Hybrid System as Drug Carriers

The development of advanced materials from the combination of macromolecules with inorganic species has become one of the most innovative research fields. Following this approach, the synthesized hybrid materials allow the tailoring of properties from the atomic to the mesoscopic and macroscopic length scales. This ability to control materials' properties over broad length scales suggests that research on hybrids can have a significant impact in diverse fields, such as nanoelectronics, separation techniques, catalysis, smart coatings, sensors, immobilization of enzymes, biomedical and polymer composite applications. The organic-inorganic hybrid materials diverse into many forms, such as composite film, gel, particle.

To obtain functional hollow polymer spheres, various methods have been reported, which are categorized as self-assembled formation, template approaches, and complex approaches, such as emulsion polymerization, where use of a soft template coexists with self-assembled layer formation. Based on these synthetic approaches, hybrid types of capsules have also been extensively developed. The major routes for fabrication are inorganic layer formation on hard and soft templates or starting with an inorganic particle template on which to form the organic layer. Yan E. [12] have fabricated an Hybrid hollow nanospheres of chitosan–silica templated by chitosan–poly(acrylic acid) nanoparticles in a complete aqueous system, which provide a pH-sensitive switch in physiological and sub-cell environments for the release of loaded drug.

The hybrid hollow nanospheres show high surface area and pore volume. DOX can be efficaciously incorporated inside the hybrid nanospheres and released slowly at physiological condition but released more rapidly in suitable intracellular environments. This material should have a potential application in construction of site-selective, pH-sensitive drug delivery systems.

Takahashi T. [42] has prepared a PEG–clay hybrid in aqueous media using a PEG/polyamine block copolymer. The dispersion stability of high ionic strength was remarkably improved by surface modification with PEG. Improvement of the stability depends on the shielding of the negative charge of the clay nanocrystals due to the coordination between the clay surface and amino groups in the side chain of the PAMA segment, and the nonionic and hydrophilic features of the PEG segment. These results obtained here satisfy some of the pharmaceutical requirements, for example, as a drug carrier for sustained release as well as for the improvement of bioavailability. Also, the acetal group on the perifery of the nanocrystals can easily be hydrolyzed to an aldehyde group by acid treatment. Thus, it might be utilized as a ligand binding site. These results strongly suggest that the PEG-modified porous clay is anticipated to be an advanced drug carrier not only for sustained release but for targeted DDS material by modification with ligands for the target molecules or organs.

Paul G. [43] has developed organic-silica based drug carriers by sol-gel techniques for the controlled release of drug. Two drug molecules, Propranolol and Persantin, have been

encapsulated by a sol-gel process in an organic-inorganic hybrid matrix by in situ self-assembly. In this self-assembled sol-gel synthesis, the nature of guest-host interactions and pore structures is dictated by the synthetic parameters, pH values, and composition. The drug release increases above and below the charge matching pH regime which is centered around the isoelectric point of silica. The alkyl/aromatic substitution in the silica gels imparts hydrophobic character to the gel which controls the surface interactions of the drug as well as the diffusion barriers of the matrix. Spray drying of the self-assembled sol leads to an enhanced dissolution process. The controlled drug release achieved from the sol-gel silica systems can be further developed and applied into the large library of newly discovered drugs.

1-2-3 Cellular Delivery of Nanoparticles

Cellular delivery involving the transfer of various drugs and bio-active molecules (peptides, proteins and DNAs, etc.) through the cell membrane into cells has attracted increasing attention because of its importance in medicine and drug delivery. This topic has been extensively reviewed. The direct delivery of drugs and biomolecules, however, is generally inefficient and suffering from problems such as enzymic degradation of DNAs. Therefore, searching for efficient and safe transport vehicles (carriers) to delivery genes or drugs into cells has been challenging yet exciting area of research [54]. In past decades, many carriers have been developed and investigated extensively which can be generally classified into four major groups: viral carriers, organic cationic compounds, recombinant protiens and inorganic

nanoparticles. Many inorganic materials, such as calcium phosphate, gold, carbon materials, silicon oxide, iron oxide and layered double hydroxide (LDH), have been studied. Inorganic nanoparticles show low toxicity and promise for controlled delivery properties, thus presenting a new alternative to viral carriers and cationic carriers. [44, 45] To aid our understanding of the surface properties, functionalisation of nanoparticles and their biointeractions, it is useful to conceptually develop some generic scenarios of nanoparticles and biomolecular interactions. Figure 1.1 is a schematic representation of surface-functionalised inorganic nanoparticles, and the processes of biomolecule uptake and the cellular transfer pathways [46].

There are a large number of inorganic nanoparticles that can be potentially used as carriers for the cellular delivery of various drugs including genes and proteins. However, most inorganic nanoparticles have to be subjected to chemical and/or biological modification to meet the stringent requirements for cellular delivery, such as good biocompatibility, strong affinity between the carriers and biomolecules, high charge density of the hybrids, site-specificity, etc. The functionalisation or modification depends, to a large degree, on the types of nanoparticles that provide specific functional groups on the surface, as summarized in Table 1.1. For instance, silica nanoparticles are usually modified with silane species while gold nanoparticles are modified with thiol groups. Carbon materials can have many surface functional groups, but –COOH is often used to react with NH_2– to anchor the organic

modifier.

The organic molecules used to functionalise inorganic nanoparticles usually have two feature groups: the anchoring group and the charging group, as listed in Table 1.1.as shown in Step 1 of Figure 1.1. The former anchors itself onto the surface of nanoparticles while the charging group binds with the biomolecules and also imparts the positive charge to the hybrid nanoparticles. For example, *N*-(2- aminoethyl)-3-aminopropyl-trimethoxysilane is a suitable modifier for silica nanoparticles [47, 48] in which methoxysilane (Si-OCH_3) acts as the anchoring group and amino group as the charging group. When amino groups are protonated at pH = 7.4, the modified nanoparticles are positively charged and bound with the DNA chain via electrostatic interactions. Similarly, thiol (–SH) is a good anchor on gold nanoparticle surface [49]. In fact, the charging group, usually amino ($–NH_2$), imino (–NH–) and/or =N–, is readily protonated under the physiological condition (pH = 7.4) and thus positively charges the nanoparticles. Further modification involves the grafting of some other functional groups for specific cells or sites targeted delivery.

2. Experimental Section

2-1 Chemicals and Reagents

1. Chitosan (Mw=215000g/mol, deacetylation degree=85-90%, Aldrich-Sigma)
2. 2-propanol (Sigma Co.)
3. Sodium hydroxide (Sigma Co.)
4. chloroacetic acid (Sigma Co.)
5. hexanoyl anhydride (Sigma Co.)
6. (3-Aminopropyl)triethoxysilane) (APTES, purity>98%, Fluka)
7. 1-Ethyl-3-(3-dimethylaminopropyl) carbodiimide methiodide (EDC, Sigma-Aldrich)
8. Dialysis tubing cellulose membrane (M.W.12400，avg. flat width 33 mm, Merck)
9. Fluorescein isothiocyanate (FITC, Sigma)
10. (S)-(+)-camptothecin (95%, CPT, Sigma)
11. Dimethyl sulfoxide (DMSO,Scharlan)
12. Phosphate buffered saline (PBS, UniRegion Bio-tech)
13. Dulbecco's modified Eagle's medium (DMEM, Gibco)
14. Ham's F12 medium (GIBCO)
15. L-glutamine (Sigma)
16. HEPES(GIBCO, Invitrogen^{TM} cell culture)
17. Sodium pyruvate (100Mm, Gibco)

18. Fetal bovine serum (FBS, Sigma)

19. Trypsin EDTA (Sigma)

20. Trypan blue (Sigma)

21. 3-(4,5-dimethylthiazol-2-yl)-2,5-diphenyltetrazolium bromide(MTT reagent)

22. Trixon (J.T.Beker)

23. Formaldehyde (Riedel de Haen)

24. Fluorescence mounting medium (Dako)

25. 4'-6-Diamidino-2-phenylindole (DAPI, Invitrogen)

26. Rhodamine-Phalloidin (Invitrogen)

2-2 Apparatus

1. Solid-State Nuclear Magnetic Resonance(Bruker DSX400WB NMR spectrometer, Germany)
2. Fourier Transform Infrared Spectroscopy (FT-IR, Unican Mattson Mod 7000)
3. Scanning Electron Microscopy（SEM 6500, JEOL2100, Japan）
4. Transmission Electron Microscopy(TEM, JEOL2100, Japan)
5. Dynamic Light Scattering(BI-200SM Goniometer DLS, Brookhaven Inc., Holtsville, NY)
6. X-ray diffractometer(XRD, M18XHF, Mac Science, Japan)

7. Flow cytometry(Becton Dickinson, USA)
8. Thermogravimeic Analyzer(TGA, TA Instrument Q500)
9. Fluorescence Microscopy(eclipse, TE2000-U, Nikon)
10. Confocal Laser Scanning Microscopy(D-eclipise C1, Nikon)
11. UV-vis spectrometer(Evolution 300, Thermo)
12. ELISA(DV990BV4,GDV)
13. Incubator(NUAIRE)
14. Autoclave(TOMIN)

2-3 Synthesis of Amphiphilic Silica-CHC Hybrid Molecules

2-3-1 Tetraethylorthosilicate(TEOS) as the precursor

Once the amphiphilic CHC was successfully prepared through both hydrophilic carboxymethyl and hydrophobic hexanoyl substitutions, the resulting amphiphilic CHC was then further chemically modified with the incorporation of silane precursor. A small amount, 1 g, of CHC was first dissolved and dispersed in 50 mL of D.I water (0.5 wt %) under vigorously agitation at room temperature for 24 hours until the CHC was fully dissolved. Aliquots of 4.071g of Tetraethylorthosilicate(TEOS) silane coupling agent was added into the CHC solution, and then add HCl to adjust the pH value to pH2~4. The mixture was gently stirred to avoid air interference and all the reactions were performed under a N_2 atmosphere to

ensure a well reaction control of the TEOS with the CHC, and prevent undesired reaction from being contact with moisture[28]. After 24-h reaction, the resulting mixture was collected by dialysis membrane with ethanol /water solution (75%v/v) for 24 hours and following with ethanol solution for 24 hours. The resulting powder, with white appearance, was obtained after evaporation and drying overnight in an oven at 50℃.

2-3-2 (3-aminopropyl)triethoxysilane silane(APTES) as the Precursor

2-3-2-1 Control the molar ratio of (NH_2 group of APTES)-to-(COOH group of CHC)

As aforementioned, once the amphiphilic CHC was successfully prepared through both hydrophilic carboxymethyl and hydrophobic hexanoyl substitutions, the resulting amphiphilic CHC was then further chemically modified with the incorporation of silane precursor. A small amount, 0.25 g, of CHC was first dissolved and dispersed in 50 mL of D.I water (0.5 wt %) under vigorously agitation at room temperature for 24 hours until the CHC was fully dissolved. Through the generally molar ratio measurements, aliquots of 160μL of (3-aminopropyl)triethoxysilane silane coupling agent was added into the CHC solution, taken as the molar ratio of (NH_2 group of APTES)-to-(COOH group of CHC) was 1:1, and0.012g of EDC as catalyst was also added[17]. The mixture was gently stirred to avoid air interference [28](incorporated as small bubbles), after 24-h reaction, the resulting mixture was collected by dialysis membrane with ethanol /water solution (75%v/v) for 24 hours and following with

ethanol solution for 24 hours. The resulting powder, with white-yellow appearance, was obtained after evaporation and drying overnight in an oven at 50℃.

2-3-2-2 Control the reaction time

In order to figure out how the reaction time affects the resulting hybrid molecule, the reaction time was controlled. After APTES and EDC were added into the CHC solution, 8hr, 24 hr and 48hr of the reaction time was applied.

2-3-2-3 Control the added amount of the catalyst, EDC

To figure out the sufficient amount of the catalyst was added or not, the added amount of EDC was controlled, the experimental process and the method were remain the same.

2-4 Symbol Number

Tetraethylorthosilicate(TEOS) as the precursor

"CHC-TOES" was used as the symbol for hybrid which synthesized through CHC and TEOS. The results were discrepancy with our expectation, therefore, no further exploration and discussion were focus on the CHC-TEOS hybrids.

(3-aminopropyl)triethoxysilane silane(APTES) as the Precursor

Symbol Number	The amount of CHC (mg/mL)	The amount of APTES (μ L)	Calculated (COOH of modified chitosan: NH_2 of APTES)
C0.5A	0.5wt%(0.25g in 50 mL D.I water)	80	1: 0.5
CA	0.5wt%(0.25g in 50 mL D.I water)	160	1:1

C2A	0.5wt%(0.25g in 50 mL D.I water)	320	1:2
C5A	0.5wt%(0.25g in 50 mL D.I water)	800	1:5
C10A	0.5wt%(0.25g in 50 mL D.I water)	1600	1:10

2-5 Preparation of self-assembly silica-CHC nanocapsules

The silica-CHC sample was suspended in distilled water under gentle shaking at 25℃ for 24h, followed by ultrasonication using a probe type sonifier(Automatic Ultrasonic Processor UH-500A,China) at 30W for 30 seconds. The sonication was repeated three times to get an optically clear solution. To inhibit the heat buildup during sonication, the pulse function was used(pulse on 5.0s; pulse off 1.0s).

2-6 Characterization of the silica-CHC Molecules

2-6-1 Fourier Transform Infrared Spectroscopy (FT-IR)

The FT-IR spectra of KBr pellets were recorded (32 scans with a resolution of $4cm^{-1}$) on a Unican Mattson Mod 7000 FTIR.

2-6-2 ^{13}C- and ^{29}Si- Solid State Nuclear Magnetic Resonance

The chemical structure analysis of the hybrid molecule was characterized by nuclear

magnetic resonance (NMR). (^{13}C and ^{29}Si solid-state NMR spectra were recorded at 79.49 and 100.62 MHz, on a (9.4T) Bruker DSX400 WB NMR spectrometer).

2-6-3 Thermogravimetric analysis (TGA)

The dynamic weight loss test of hybrids macromolecules were conducted on a DuPont 2050 thermogravimetric analyzer. All tests were conducted in a N_2 purge gas using sample weights of 5~7mg over a temperature range 30℃ to 600℃ at a scan rate of 10℃/min.

2-6-4 Self-assembly Behavior (CAC concentration)

Pyrene has been frequently chosen as a fluorescence probe to monitor the self-aggregation behavior of surfactants and polymers because of its high chemical affinity to those hydrophobic microdomains. Pyrene molecule emits only small fluorescence intensity in the polar environments (for example: water) due to its poor solubility, but strongly emits when the hydrophobic microdomains are evolved in an aqueous solution. In measurement, the intensity ratio of the first peak (372 nm) and the third peak (385 nm), i.e., $I_{372}/I_{385,}$ in its fluorescent spectrum is used since this ratio has been verified to be relatively sensitive to the environment surrounding the pyrene molecules and has been frequently used as an indicator for the stable change of its surrounding environments. Pyrene-containingsolution (1.0×10^{-4} M) in methanol was added into the test tube and evaporated under nitrogen gas to remove the solvents. Then, solutions of hybrid nanoparticles in D.I water were added into the above test tube, bringing the final concentration of pyrene to 1.0×10^{-6} M, which was nearly equal to the solubility of

pyrene in water at 22℃. The mixture were sonicated for 30 min in an ultrasonic bath and shaken in a shaking air bath for 1 hour at ambient temperature. Pyrene emission spectra were obtained using a fluorescence spectrophotometer (Hitachi FL-4500, Japan). The probe was excited at 343 nm, and the emission spectra were recorded in the range of 350-500nm at an integration time of 1.0 s. The excitation and emission slit opening were 10 and 10 nm, respectively.

2-6-5 Morphology (Scanning Electron Microscopy, Transmission Electron Microscopy)

The morphology of the self-assembly hybrid nanoparticles were examined by field-emission scanning electron microscopy(FE-SEM, JAM-6500F). The microstructure observations were performed using transmission electron microscope(TEM, JEOL2100, Japan) operated at 200keV.

2-6-6 Dynamic Light Scattering(DLS) Analysis

The mean size and size distribution of the self-assembly hybrid nanoparticles were measured by *dynamic light scattering*(BI-200SM Goniometer DLS, Brookhaven Inc., Holtsville, NY).

2-6-7 Swelling Ratio

The swelling ratio of the self-assembly hybrid nanoparticles were primary determined by the comparison of the particle size under the SEM image with the mean size measured by the

dynamic light scatter (DLS).

2-6-8 Zeta potential

The zeta potential of the self-assembly CHC and the hybrids nanoparticles were measured by Delsa^{TM} NanoC. Particle Analyzer.

3 Characterization, Analysis and Discussion

3-1 The effect of different silane precursor on the hybrid molecules

In order to synthesis the chitosan-silica hybrid molecule, two types of silane precursors have been test, and the ^{13}C-, ^{29}Si- solid state nuclear magnetic resonance (solid-state NMR) was used to estimate if the siloxane groups were grafted with chitosan main chain or not.

3-1-1 Tetraethylorthosilicate(TEOS) as the precursor

Herein, tetraethylorthosilicate(TEOS) was also used for the preparation of the silica-CHC hybrid molecule, as mentioned in the experimental section, the pH value and the reaction time were also adjust to the most suitable environment. The initial idea was that the siloxane groups of TEOS hydrolysis under the acidic environment and then combine with the COOH groups of the modified chitosan. However, through the analysis of ^{13}C- and ^{29}Si- solid state NMR, it indicated that the siloxane groups was preferrentially hydrolyzed and condensed with each other rather than connected with the modified chitosan, and, hence, formed bulky silica network. From the ^{29}Si-NMR spectra, Figure 3.1, there are three characteristic peaks shown at Q_2,Q_3,Q_4…. ppm, which was represent $Si(OSi)_2(OH)_2$, $Si(OSi)_3(OH)$, $Si(OSi)_4$, indicated that the most of the siloxane groups were condensated and formed the silica network, and none of the Si atom was connected with the organic group(Carbon atom). From the data, we estimate

that it's failed to connect the inorganic silica part with the modified chitosan via the use of tetraethylorthosilicate(TEOS) as the precursor.

3-1-2 (3-aminopropyl)triethoxysilane (APTES) as the Precursor

Qualitative Analysis

Figure 3.2a shows the ^{13}C solid state NMR spectra of neat CHC and the CA hybrid. For the hybrids, the linkage of the siloxane to the CHC polymer is confirmed by the appearance of new signals at ca. 11, 23, 44 and 160-170 ppm. The peaks located at near 11, 23, and 43 ppm are characteristic peaks of the $(CH_2)_3$ aliphatic chains and the ester group carbons bonded to silicon atoms (-Si-CH_2CH_3). The peak at around 164 ppm due to C=O amide functions is clearly evidenced in all the spectra [9,13,14]. This observation supports the incorporation of inorganic lattice with the organic CHC macromolecule where the carboxylic acid of the CHC is chemically coupled with the $–NH_2$ group from the the silane. The chemical reaction of the modified chitosan with the APTES was schematically shown in Scheme 3.1.

Figure 3.2b shows the ^{29}Si solid state NMR spectra of the hybrid. The hybrids exhibit characteristic signals of T_1 (-48 to -50 ppm), T_2 (-58 to -59 ppm), T_3 (-66 to -68 ppm) [9,15,16]. These sites are labeled using the conventional T_n notation, where n (n=1, 2, 3) is the number of Si-bridging oxygen atoms, which represents the –Si in different environments. The spectra indicated the hybrids were dominated with the T_2 and T_3 environments (at -59 and -68 ppm,

respectively) indicating the presence of two main types of local structures: $(SiO)_2Si(CH_2)_3OH$ and $(SiO)_3Si(CH_2)_3$, respectively. The small peak at ca.-48 ppm is ascribed to T_1 site, which is translated as $(SiO)Si(CH_2)_3(OH)_2$ structure. Therefore, it is clear that the silica lattice chemically attached with the CHC chain is virtually a mixture of small amount of Si-OH and large population of Si-O-Si groups. From the T_2 and T_3 structures of the ^{29}Si-NMR spectra, it is reasonably to conclude that the siloxane groups (Si-OH) were subsequently condensated to form Si-O-Si network. The degree of condensation will be discussed in the next section.

The results of the ^{13}C- and ^{29}Si-NMR shown that through the carbodiimide coupling reaction, the NH_2 groups of APTES precursor was successfully connect with the COOH groups of modified chitosan(CHC) and, hence, the modified chitosan-silica hybrid molecule was formed. The further semi-quantitative analysis of the hybrid molecules will be discussed in the next section.

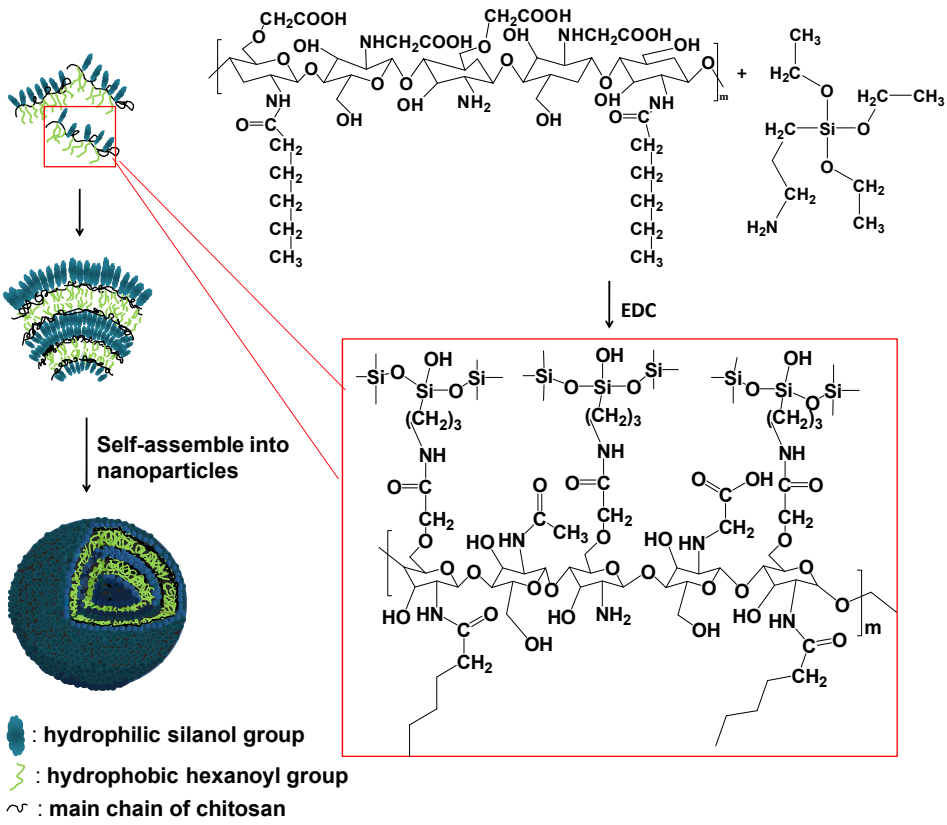

Scheme3.1

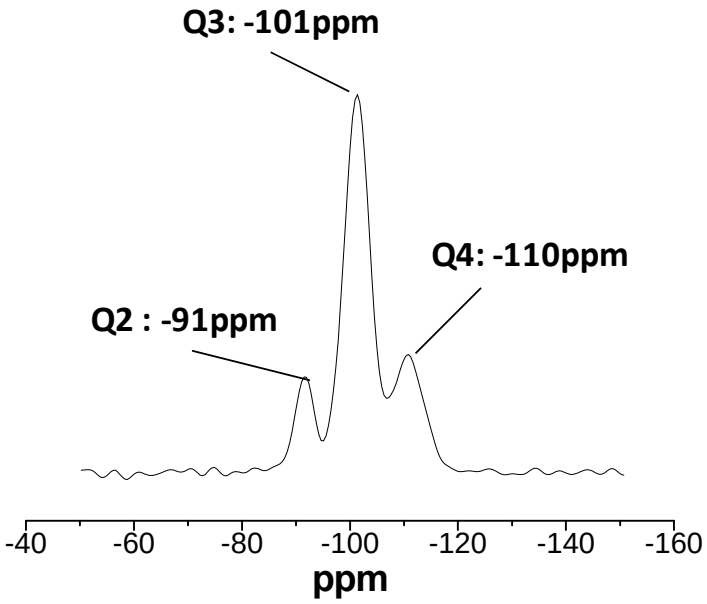

Figure3.1 The ^{29}Si-solid state NMR spectra of CHC-TEOS

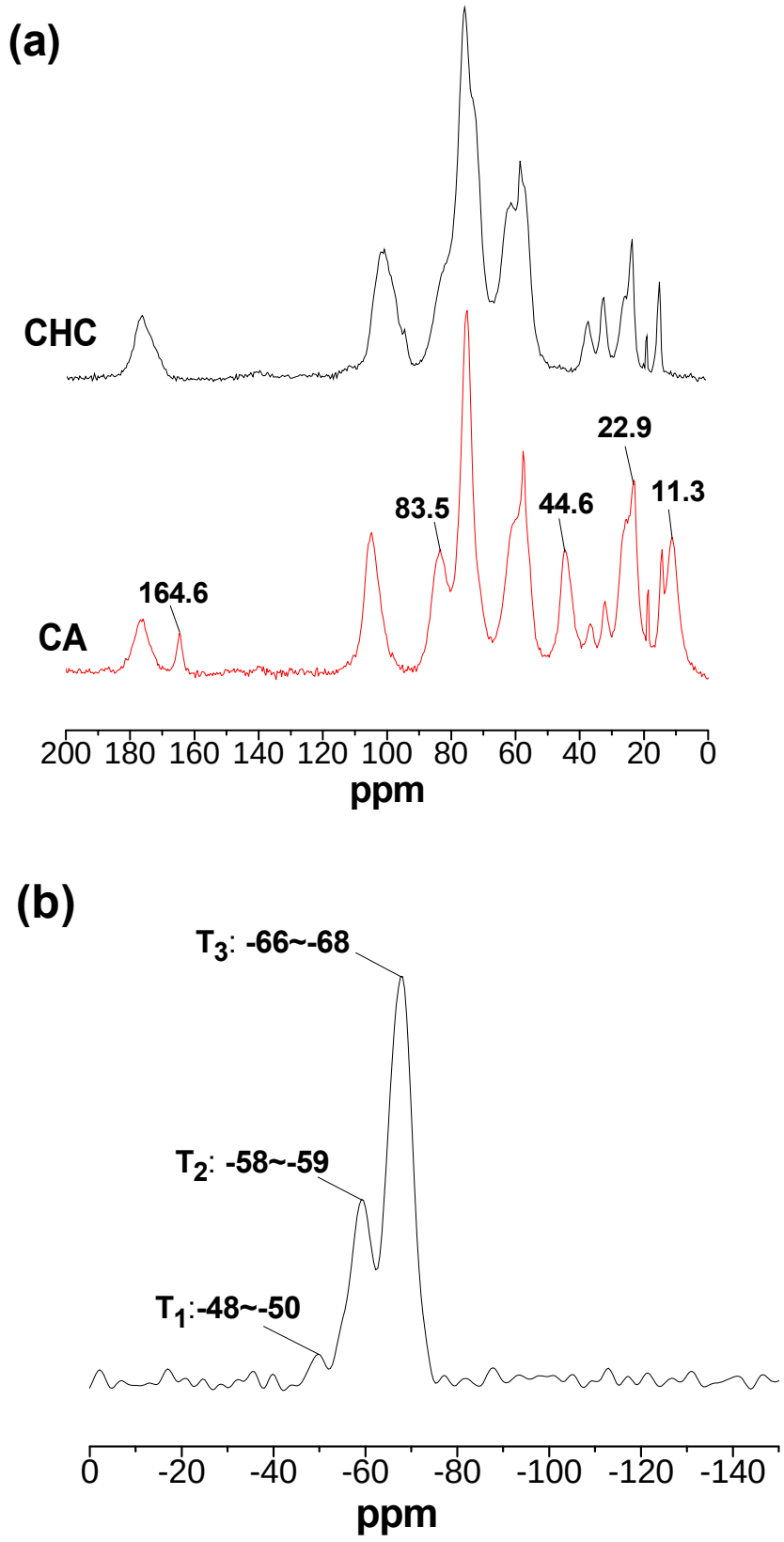

Figure3.2 (a) ^{13}C solid state NMR spectra of CHC and silica-CHC(CA)

(b) ^{29}Si solid state NMR spectra of silica-CHC

3-2 The physical and chemical properties of the silica-CHC hybrid molecule

3-2-1 Fourier Transform Infrared Spectroscopy (FT-IR)

As aforementioned in the NMR analysis, through the use of APTES silane, the silica-CHC hybrid molecules can be successfully synthesized. The hybrid was prepared through the carbodiimide coupling reaction, where the carboxylic groups from the carboxymethyl ligands of the CHC is expected to chemically react with the amide group ($-NH_2$) of the APTES precursor. On the other hand, with the used of tetraethylorthosilicate(TEOS), the siloxane groups were hydrolyzed and condensedn with each other rather than connected with the modified chitosan, hence, failed to synthesize the silica-CHC hybrid molecule. The chemical structure of the hybrid molecules was characterized by FTIR, as illustrated in Figure 3.3, The presence of C=O stretching bands near 1720 cm^{-1} and a peak near 1200 cm^{-1} assigned to the CO single bond. The absorption band at 2700-3300 cm^{-1} is referred to the stretching mode of OH group in the CHC which became broader than that in silica-CHC (hereinafter termed as CA) hybrid. This may be ascribed to the OH stretching of the unmodified COOH groups along the CHC chain. After modification with the silane molecule, the absence of the peak at 1720 cm^{-1} gave supporting evidence that the carboxylic acid of CHC was replaced to a certain

extent by the silane. The displacements of the NH (1590-1560 cm^{-1}) and CO (1652-1633cm^{-1}) were shifted in the CA hybrid, which may translate as a result of the presence of urethane groups in the hybrids. Fu et al [9] reported that the regions of the urea groups vibrations, the so-called “amide I” and “amide II“, were highly complex vibrations: the “amide I” mode (1800-1600 cm^{-1}) involved the contribution of the C=O stretching, the CN stretching, and the C-C-N deformation. The “amide II” mode (1600-1500 cm^{-1}) is a mixed contribution of the in-plane N-H bending, C-N stretching, and C-C stretching vibrations. The shifts of the NH and CO peaks in CA hybrid also indicated that the “amide I” mode is predominant, revealed a chemical link between N-H and C=O groups. The presence of the peak at 2300-2360 cm^{-1} of the spectrum for the CA hybrid represents the C=N stretch vibration. The peak showed up at 900-950 cm^{-1} in the hybrids, indicated a Si-OH stretch mode displacement, revealed that the uncompleted polycondensation of the silanol groups. In other words, the hybrids synthesized are not just a polymeric Si-O-Si network structure but with some unbounded Si-OH groups exposed along the hybrid chain. In comparison, the 1000-1200 cm^{-1} band in the hybrids became broader than that at the CHC spectrum which may due to the peak of Si-O-Si (stretch mode) overlapped with the -C-O-C- glycosidic linkage of the CHC [9-11].

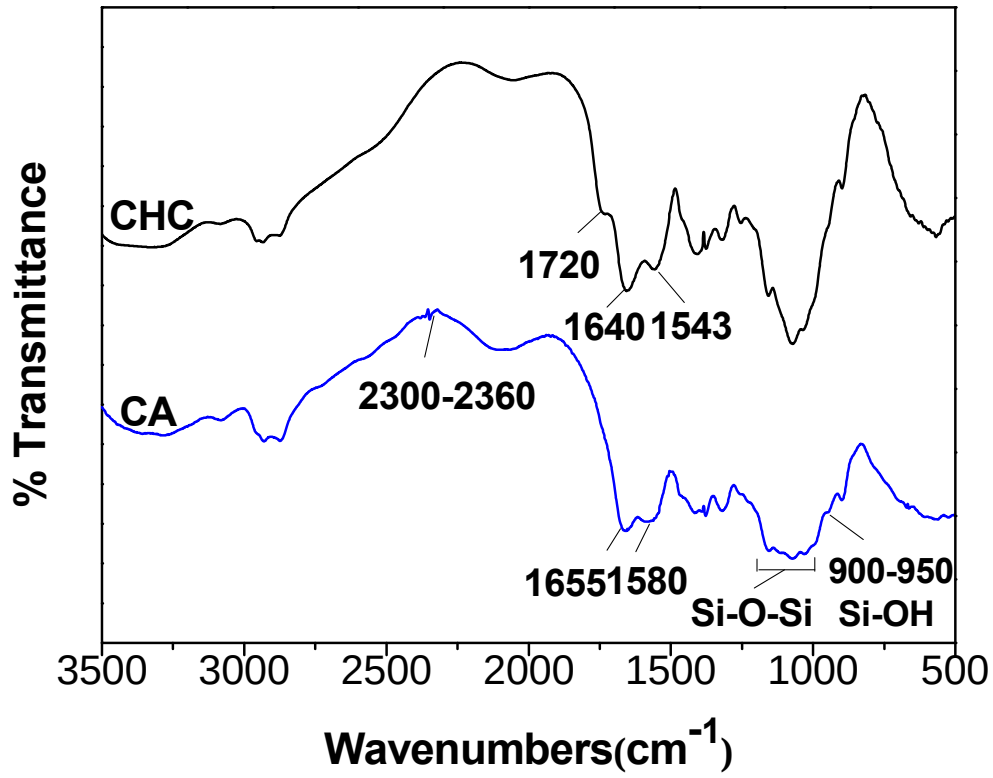

Figure 3.3. FTIR spectra of CHC and silica-CHC hybrid(CA).

3-2-2 ^{13}C- and ^{29}Si- Solid State Nuclear Magnetic Resonance

As we have mentioned in the previous section, through the qualitative NMR analysis of the hybrid molecules, we can specifically identify the chemical structure of the hybrid silica-CHC molecule. In order to understand the effect of the added amount of silane precursor on the formation of the hybrid molecule, further go through the semi-quantitative NMR analysis.

3-2-2-1 Semi-quantitative Analysis

The semi-quantitative analysis of the hybrid macromolecule was also performed by ^{13}C-, ^{29}Si-nuclear magnetic resonance, where the weight of each sample was fixed 0.29 g and the frequency was controlled at 6230 Hz. However, since the variant, such as degree of substitution, in molecular structure of the hybrids between each sample should present, together with the low natural abundance of ^{13}C, ^{29}Si nuclei, smaller gyromagnetic ratio and long T_1 relaxation time make the acquisition of quantitative spectra with adequate signal-to-noise ratio impractical. It is thus inherently difficult to precisely perform a quantitative analysis via current technical protocol in this work, instead, semi-quantitative analysis was applied.

The substitution of the siloxane group to the COOH group of chitosan main chain was calculated through the ^{13}C-NMR spectra. Since we have mentioned that the the ^{13}C-NMR spectra exhibited several resonances at 160-180 ppm, associated with carbonyl groups in different environments, the peak at 176 ppm was attributed to the COOH group of the chitosan, which was present in the CHC ^{13}C NMR spectra. After the siloxan groups grafted to the COOH groups of the chitosan and formed the CONH bond, the peak at 164 ppm appeared in the hybrid spectra. With the mole ratio of APTES: CHC increased, the growth of the peak at 164ppm and the decline of the peak at 176ppm become more and more pronounced. Through the deconvolution using Gaussian band shapes, we were able to estimate the peak

assignment and the relative population of each peak, as shown in Figure3.4. It is also assumed that the decrease in the integral area of the COOH peak was considered to be a result of the reaction toward CONH bond formation. Therefore, through estimation of the integral area of the two peaks (164 ppm and 176ppm), the increment in the area at 164 ppm was estimated and considered to be the substitution degree.

Substitution degree (%) = (the integral area of peak at 164ppm/ the integral area of peaks at 164 and 176ppm) * 100%

The Gaussian peak fitting results of each hybrid sample were illlustrated in Figure 3.4 and the estimated substitution degree was given in Table 3.1. From the ^{13}C spectra, the increase of silane precursor (APTES) molar ratio gives rise to a higher substitution.

From the qualitative analysis of the ^{29}Si-NMR spectra, we have already known that the silica lattice chemically attached with the CHC chain resulting in virtually a mixture of small amount of Si-OH and large population of Si-O-Si groups. The degree of condensation (c) involves the population of the distinct Si (T_1, T_2, T_3) environments and it was calculated using the equation,

$$c = 1/3(\%T_1+2\%T_2+3\%T_3)$$

Peak assignment and the relative population of the different Si sites, estimating after deconvolution using Gaussian band shapes, are depicted in Figure 3.5 and Table 3.2. Increase

in the molar ratio of silane precursor (APTES) (refer to the experimental section) caused an increase the population of the T_2 and T_3 sites but reduce the population of T_1 site, which is interpretated as a result of higher degree of condensation and , hence, either a more bulky silica lattice developed or a structurally more compacted network formed. The results indicated that the degree of poly(siloxane) formation varies from hybrid to hybrid with different starting silane-to-CHC ratios.

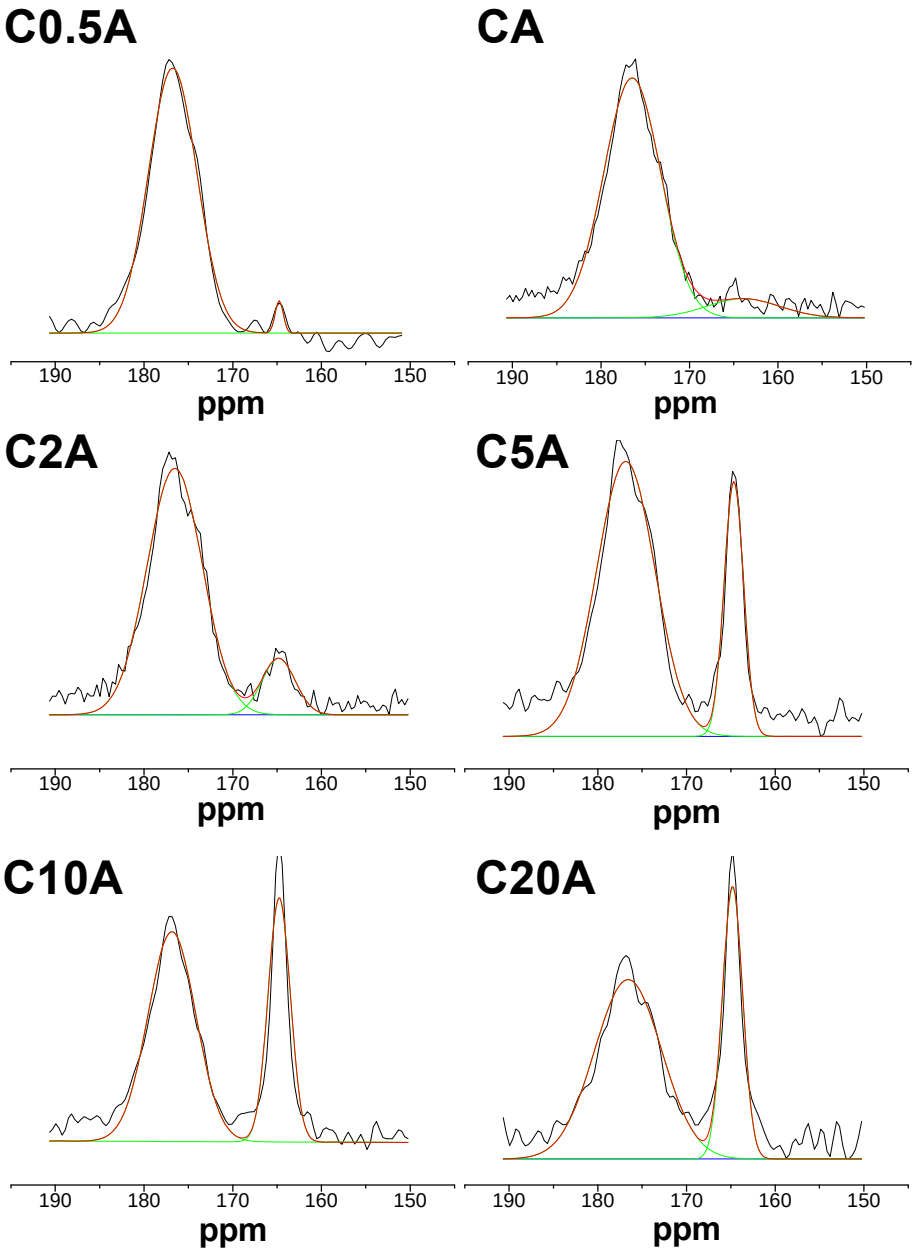

Figure3.4 Quantitative analysis of ^{13}C-NMR spectra of silica-CHC hybrid

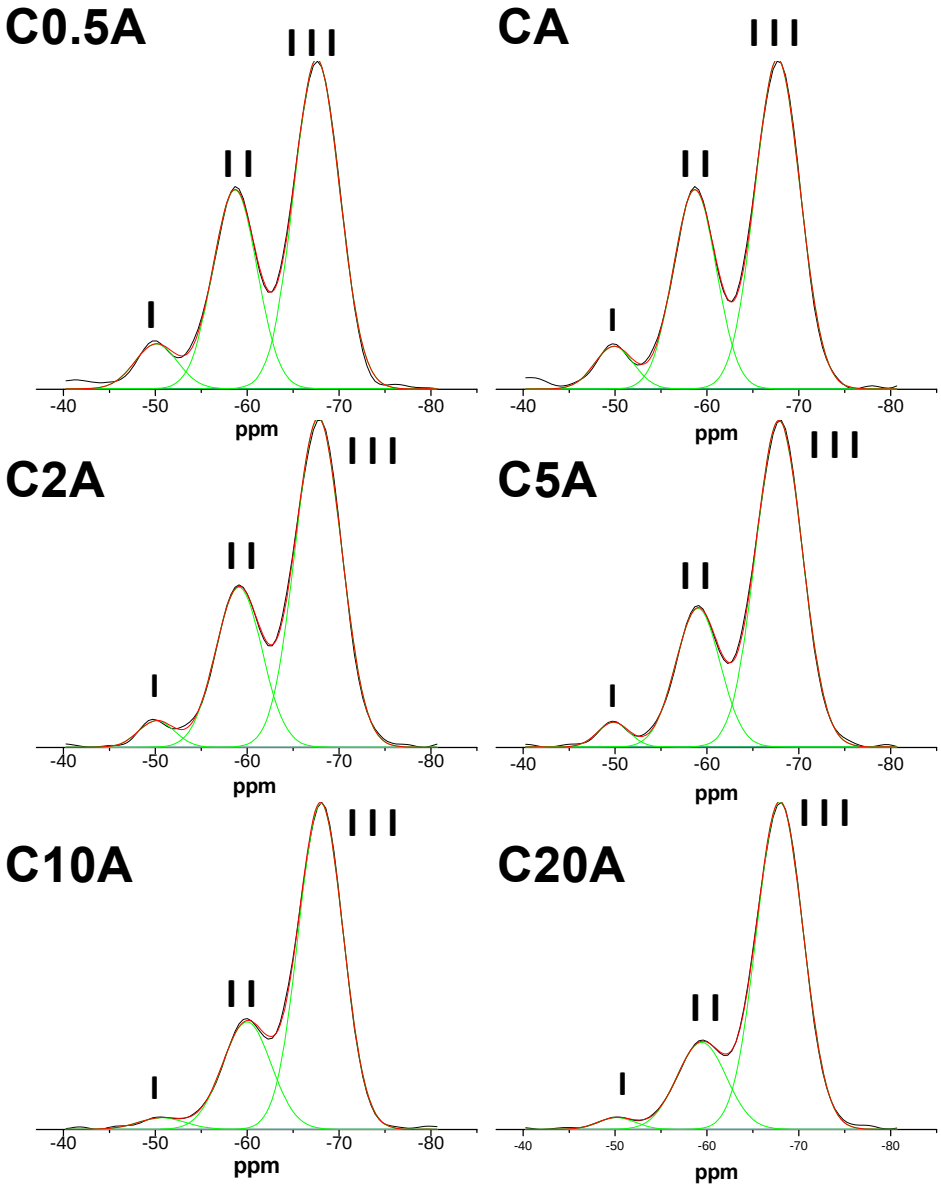

Figure3.5 Quantitative analysis of ^{29}Si-NMR spectra of silica-CHC hybrid

Sample		C0.5A	CA	C2A	C5A	C10A	C20A
Position (ppm)	164	1.98	9.24	12.05	23.5	31.3	36.8
	176	98.02	90.76	87.95	76.5	68.7	63.2
Substitution degree(%)		1.98%	9.24%	12.05%	23.5%	31.3%	36.8%

Table 3.1 The substitution degree of each hybrid sample, estimated from ^{13}C-NMR spectra.

Peak	Position(ppm)	Sample	C0.5A	CA	C2A	C5A	C10A	C20A
I	-48 ~ -50	T1: $(SiO)Si(CH_2)_3(OH)_2$	7.5%	6.6%	4.04%	3.53%	2.68%	2.2%
II	-58 ~ -59	T2: $(SiO)_2Si(CH_2)_3OH$	34.1%	34.1%	31.37%	27.87%	25.77%	21.5%
III	-66 ~ -68	T3: $(SiO)_3Si(CH_2)_3$	58.4%	59.3%	64.59%	68.6%	71.55%	76.3%
Degree of condensation, c (%)			83.67	84.25	86.85	88.35	89.63	91.35

Table 3.2 The condensation degree of each hybrid sample, calculated from ^{29}Si-NMR spectra.

3-2-2-3 Effect of the catalyst on the Hybrid synthesis

The catalyst, EDC, provided a lower chemical potential pathway to the combination of COOH group of modified chitosan to the NH_2 group of APTES precursor. However, if the amount of the EDC was not sufficient to catalyze the reaction, the NH_2 groups of APTES are not easily to combine the COOH groups of modified chitosan, and the unreacted APTES will hydrolyze and condensate quickly. In order to avoid such unwant reactions, different amount of EDC was added in order that an optimal level of the EDC can be employed in the synthesis. Figure 3.6. The degree of substitution and condensation do not have significant changes as the

amount of EDC increased 5 times and even 20 times, which was also evident that the original amount of EDC was sufficient to catalyze the reaction.

3-2-2-2 Effect of reaction time on the hybrid synthesis

As aforementioned, the substitution degree of the siloxane group to the COOH group of chitosan and the condensation degree of silica group were measured through the semi-quantitative solid state NMR analysis. The substitution degree was increased with the increased of the added amount of APTES precursor, from 1.98% to 36.8%. The condensation degree of the silica-CHC hybrid samples all reached above 80%, indicated that a large amount of the siloxane group were condensated and formed the bulky silica network, which might reduce the hydrophilic force and with the bulky groups increased, might retard the self-assembly behavior. In order to estimate if the reaction time could affect the condensation degree of the silica-CHC hybrid or not, we chose the component of CA and control the different reaction time, from 8h, 24h, to 48h. The result was shown in Figure 3.7, indicated that the reaction time does not have significant effect on the condensation degree of the silica group. With the reaction time reduced to 8 hour, the condensation degree was still keep at around 80%, indicated that the reaction time is not the dominant key-factor on the condensation process of the synthesis of silica-CHC hybrid molecules.

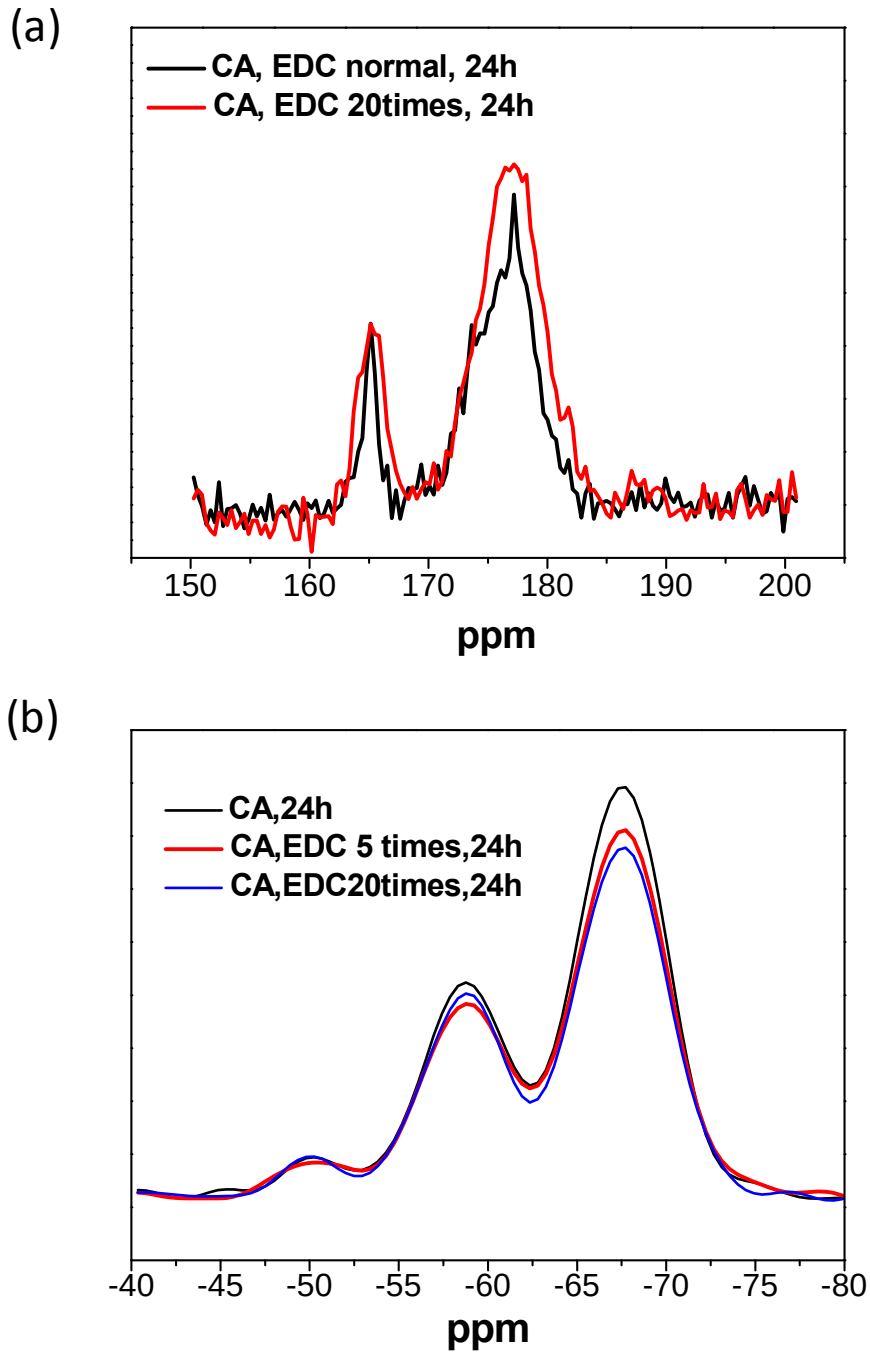

Figure3.6 (a) The solid-state ^{13}C- NMR spectra(150~200 ppm) of CA hybrid synthesized under different amount of EDC added. ***(b)*** The solid-state ^{29}Si- NMR spectra of CA hybrid synthesized under different amount of EDC added.

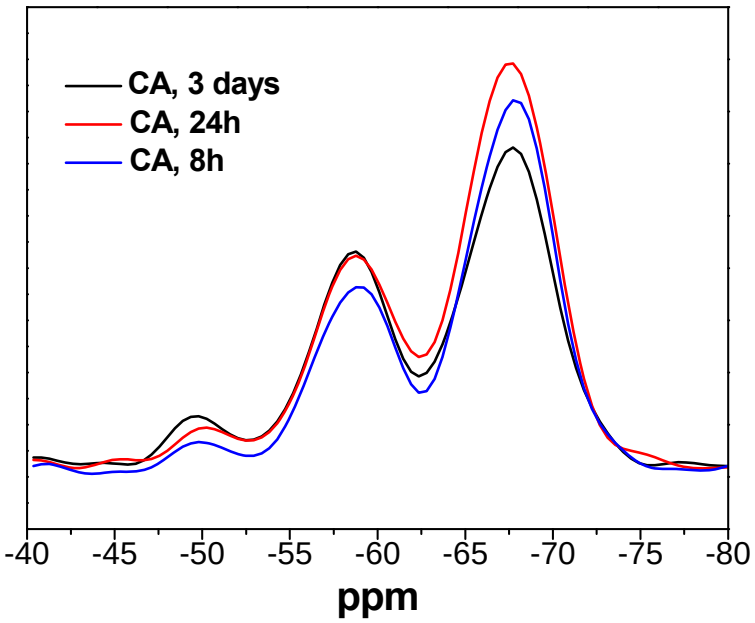

Figure 3.7 Solid-state ^{29}Si-NMR spectra of the hybrids synthesized under different reaction time.

3-2-3 Thermogravimetric analysis (TGA)

Through the thermogravimetric analysis, the ratio of the organic and inorganic can be identified. With the modify of the siloxane group on chitosan main chain, the thermal degradable temperature(T_D) should be raised due to the introduction of the inorganic group.The curve in Figure 3.9 was shifted to the higher temperature with the increased silica-to-CHC ratio, indicating that the T_D temperature was increased as the silica-to-CHC ratio increased. This indicated that the inorganic components were intimately combined with the organic groups and formed the singular hybrid macromolecules, the increased of the T_D temperature was induced by the encoring of the inorganic Si element, the needed energy to break the

3-2-4 Self-assembly Behavior (CAC concentration)

The structural development upon dispersing the hybrid molecules into water proved the self assembled nature of the amphiphilic hybrid [19,21], which is the same as that previously observed in its organic counterpart [8]. To further elucidate the CAC profile of the hybrids in water medium, pyrene was employed as a fluorescence probe, to investigate the self-aggregation behavior of the hybrid at a molecular level. Pyrene has been frequently chosen as a fluorescence probe to monitor the self-aggregation behavior of surfactants and polymers because of its high chemical affinity to those hydrophobic microdomains[23,24,25].

The critical aggregation concentration (CAC), which was defined as the threshold concentration of self-aggregate formation by intra- and/or intermolecular association, can be determined from the variation of the I_{372}/I_{385} value of pyrene in the presence of polymeric amphiphiles. Figure 3.10 illustrates the variation of I_{372}/I_{385} ratio of pyrene as a function of the concentration of the hybrids with various -COOH-to-NH_2 ratios, corresponding to CHC-to-silica ratio, ranging from 1:1 to 1:10.

The CAC value is increased with the silica/CHC ratio, and while comparing with neat amphiphilic CHC macromolecule, higher CAC values were always detected, i.e., the lowest CAC is 0.0186 mg/mL for 1:1 composition, compared with 0.01 mg/mL for neat CHC. (Figure 3.11) These comparatively higher CAC values suggested that the e substitution of $–NH_2$ (from APTES) to the -COOH of the CHC may undergo a subsequent condensation reaction, as evidenced in the Si-NMR spectrum, Figure 3.2b, where a bulky lattice along the chain is expected. The OH groups, i.e., $(SiO)Si(CH_2)_3(OH)_2$ may lead to more hydrated force with water molecules, forming hydrogen bonds, which, in turn, imparts more hydrophilic nature than the Si-O-Si network, i.e. T_3 structure. However, it is clear that from the NMR spectra aforementioned, the attached silica lattice has much less Si-OH groups than Si-O-Si groups along the hybrid chain. This may alter the hydrophobic-hydrophilic interaction originally evolved in the neat amphiphilic CHC macromolecule, with respect to water environment, as a result, subjecting to a change in self-assembly behavior, compared to neat

CHC. Moreover, the condensed bulk groups, having a form of Si-O-Si network, may also modify the self-assembled behavior of the hybrid macromolecules; which we assume that more silica substitutions, the more bulky groups exist in the hybrids, resulting in higher CAC values. This is further evidenced by the measurement of particle size using DLS data aforementioned (Table. S1).

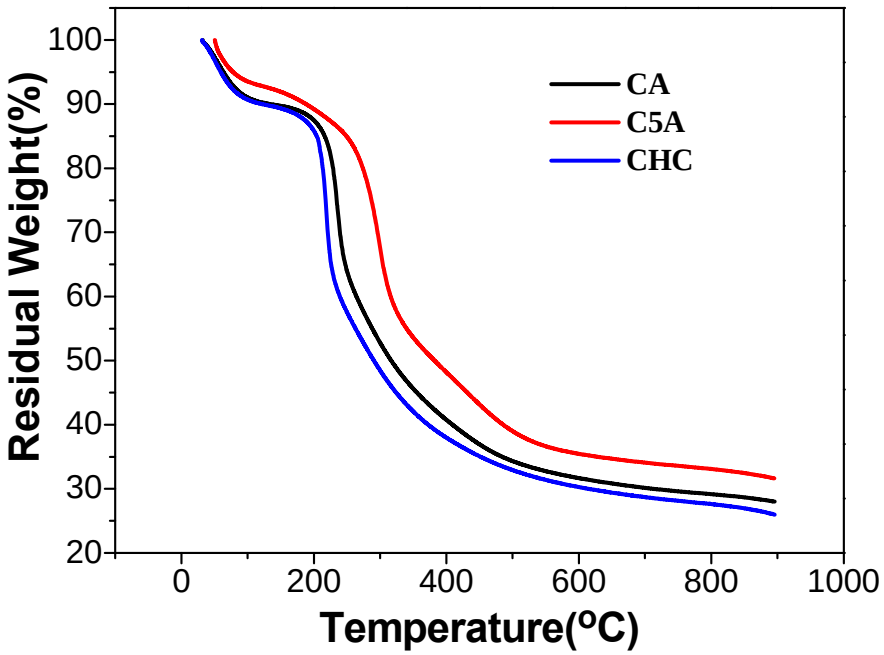

Figure 3.9 TGA analysis of CHC, CA, C5A

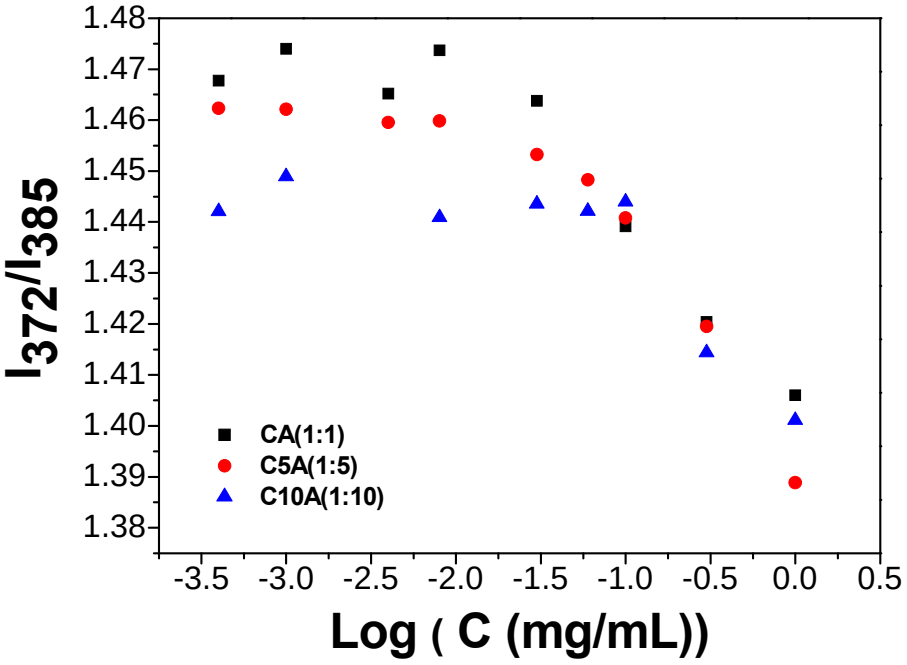

Figure.3.10 The change of I_{372}/I_{385} value of pyrene with the concentration of various composition of silica-CHC hybrids.

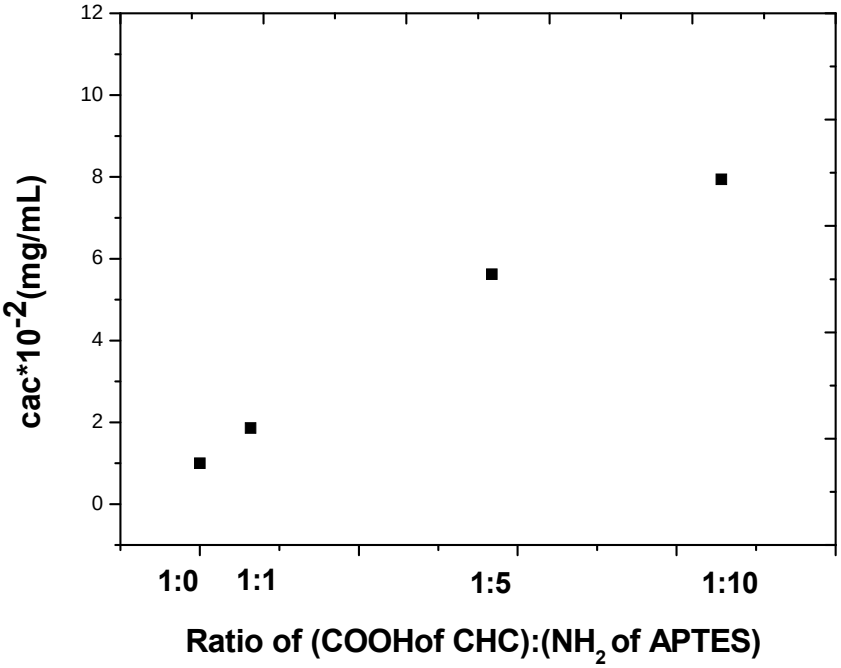

Figure 3.11 The critical aggregation concentration (CAC) of different ratio of (COOHof CHC): (NH_2 of APTES) hybrids.

3-2-5 Morphology

Scanning Electron Microscopy (SEM)

Based on both the FTIR and NMR analyses aforementioned, the molecular structure of resulting hybrids can be drawn schematically in Scheme 3.1. From the spectroscopic analyses, the siloxane group was covalently bridged to the carboxylic acid of the CHC, which was considered as a hydrophilic substitution, forming both Si-OH and Si-O-Si groups along the CHC chain, whilst the hydrophobic hexanoyl groups along the other side of the hybrid molecule remained intact. Accordingly, such a hydrophobic-hydrophilic nature imparts a self assembly force when the hybrid molecule is subjecting to an aqueous or solvent medium [19,20,21,22,27], forming a thermodynamically stable nanoarchitecture in order to minimize the free energy of the suspension system. After dissolving in D.I water, the silica-CHC hybrid molecules were found self assembling into nanoparticles, show a spherical appearance with an average size around 65 nm in diameter, as illustrated in scanning electron micrograph (SEM) image (Figure 3.12).

Transmission Electron Microscopy (TEM)

What is more than surprisingly found in this study is that the silica lattice (which has been confirmed using X-ray diffraction analysis, where a broad silica reflection peak at around 20~30° was clearly detected (Figure 3.13), after self assembly in aqueous medium, formed a highly-ordered nanophase of ~6 nm in width surrounding the nanoparticle (Figure 3.14a), for the 1:1 composition, which, to the best knowledge, has not been reported or observed before.

A layer-like nanostructure formed the hybrid nanoparticle through self assembly, where the highly-ordered silica lattice (Figure 3.14b), i.e., as a crystal layer, should be arisen due to self assembly of the hybrid macromolecule, and according to the TEM examination, such an assembly should be relatively self-organized, rather than randomly aggregated. Having amphiphilic property, the layer-like nanoarchitecture of the hybrid, also evidenced by the TEM examination, can be translated to be a result of the hydrophobic-hydrophilic arrangement. Upon such an arrangement, regions of hydrophobic nature, i.e., hexanoyl groups, are assembled and those with hydrophilic nature, i.e., silica lattice, were fused into the layer-like configuration. This arrangement also suggests that the crystal silica nanophase is atomically directed as a result of the hydrophobically-induced assembly of each single hybrid macromolecule in a well-regulated manner. Such a silica nanolayer not only reinforces the resulting nanoparticles but also renders an irreversible character of the nanoparticles from undesirable disassembly while the concentration is below the CAC, this was evidenced from an extreme dilution, i.e., greater than 10 times below the CAC, of the suspension prepared for TEM observation. This finding has its clinical significance of being diluted in circulation while being administrated for medication, which ensures retaining of the encapsulated drug from unwanted loss as a result of significant structural swelling and rupture upon a progressive dilution in blood vessel. Comparing with existing chitosan-based hybrid composites where a cross-linker, which is unlikely friendly to human, is frequently required to

stabilize the resulting assembled nanoobject, the hybrid nanoparticles developed in this study do provide unique potential for biomedical application.

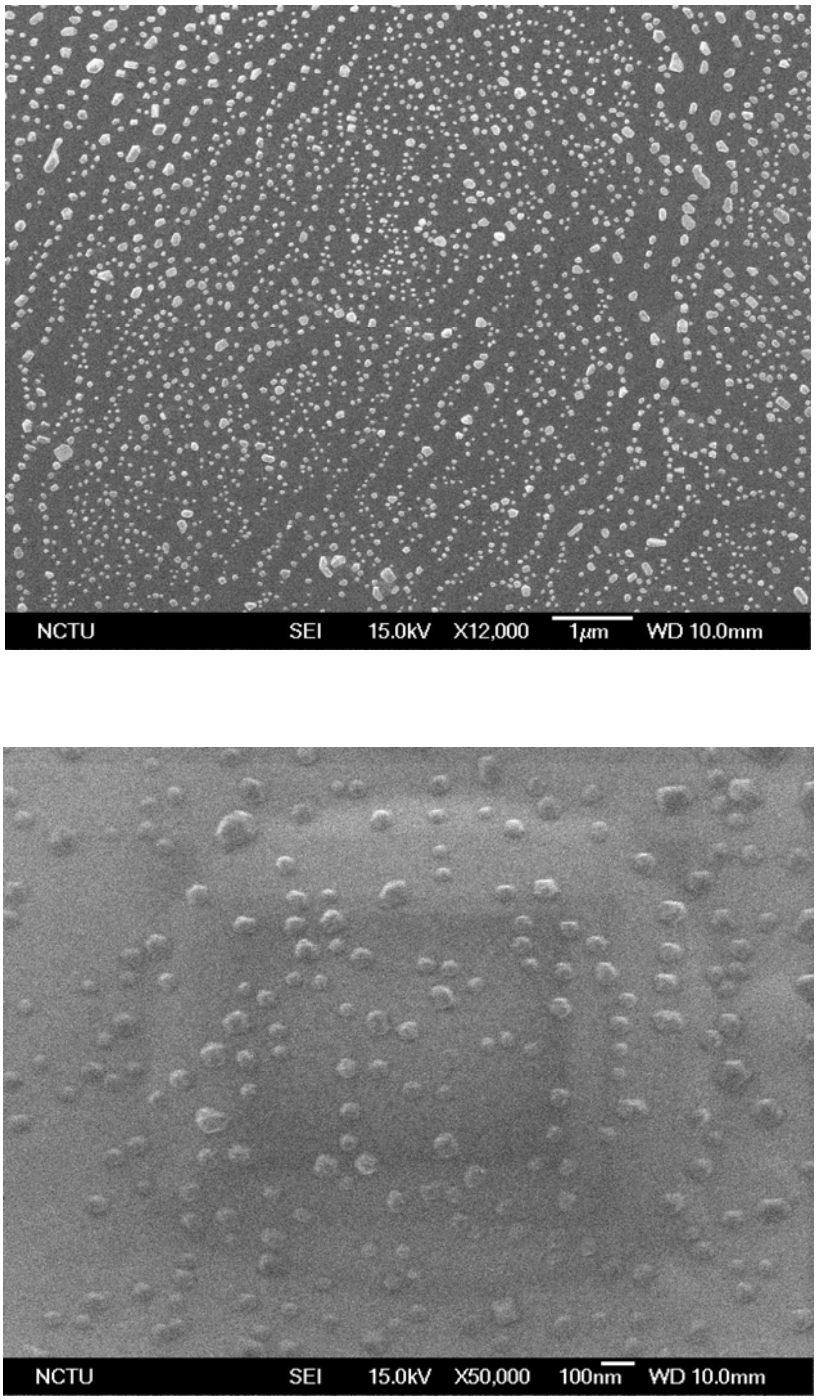

Figure3.12 SEM image of silica-CHC, the size of the nanocarriers were around 65nm.

3-2-6 The Mean Size, Zeta Potential and Swelling Ratio

The mean size of the hybrid nanoparticles was measured by dynamic light scatter (DLS). As aforementioned, with the increase of silica substitutions, the more bulky groups exist in the hybrids, which may hinder the self-assemble behavior, resulting in higher CAC values and larger nanoparticle size, shown in Table 3.3. The zeta potential of CHC and the hybrids nanoparticles was also shown in Table3.3.

The swelling ratio was primarily estimated by comparing the size under SEM image with the size measured by dynamic light scatter (DLS). The self-assembly silica-CHC nanoparticles show a spherical appearance with an average size around 65 nm in diameter in SEM images. Besides, from the dynamic light scattering (DLS) measurement (Table 3.3), the mean size of the hybrid nanoparticles was around 133 nm in diameter, which is greater by about 2 times in volume than that of SEM measurement. This is mainly due to swelling effect in water medium. In comparison with neat CHC, where a swelling of nearly 8 times was observed in an earlier study [8], indicating a considerable reduction in the swelling behavior, to nearly 4 times, when an equivalent amount of the -NH_2 groups from the APTES was chemically modified with the –COOH groups of the CHC macromolecule. Such a silica substitution should enhance the rigidity of the resulting hybrid entity, thus, reduce considerably its swelling.

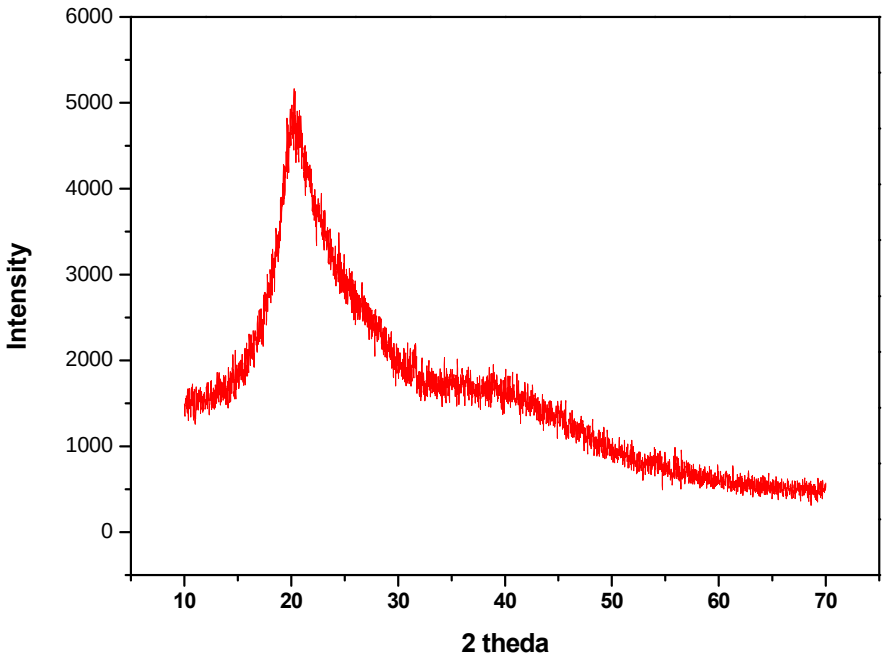

Figure 3.13 X-ray diffraction pattern of silica-CHC.

sample	mean size	Zeta potential(mV)
CHC	122	-33.47
CA	133	17.59
C2A	302	34.78
C5A	500	45.26
C10A	600	--

Table 3.3 The mean size and zeta potential of the different ratio of (COOH of CHC): (NH_2 of APTES) hybrids.

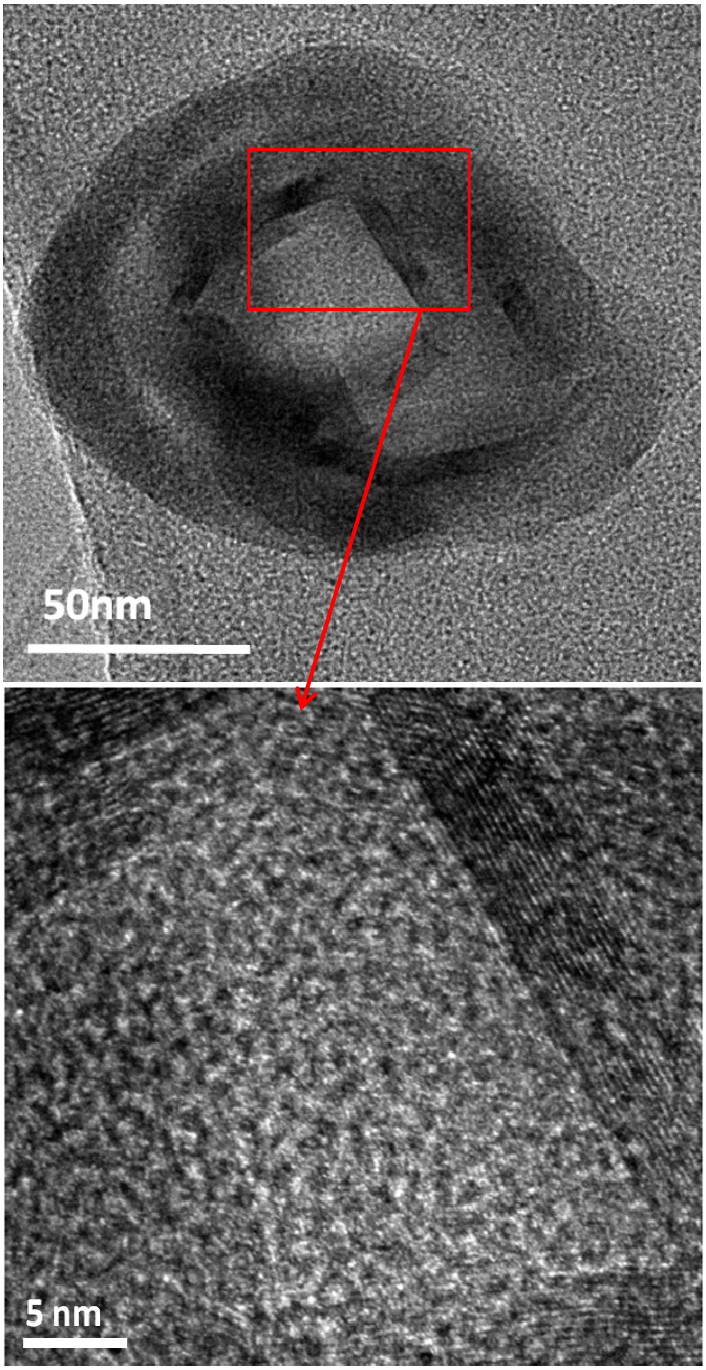

Figure 3.14 (a) TEM image of the silica-CHC nanoparticle (b) The interior TEM image of silica-CHC nanoparticle, showing a layer-like nanoarchitecture where a highly- ordered silica phase of ~6 nm in width surrounding the nanoparticle.

Conclusions

A novel hybrid macromolecule based on a chemical modification along the –COOH groups of amphiphilic chitosan (CHC) with (3-aminopropyl) triethoxysilane molecules was successfully designed and synthesized. This hybrid macromolecule showed a concentration-dependent self-assembly behavior making a final hybrid nanoparticle tunable in size, drug encapsulation efficiency and release profile. Formation of a highly-ordered crystalline silica layer of ~6 nm in thickness, upon self-assembly of the hybrid molecule rendered a prolonged, sustained release of a model drug, CPT, compared with the neat CHC molecules. Such an continuous highly-ordered silica nanoarchitecture evolved surrounding the hybrid nanopartciles provided not only a well-stabilized nanostructure without using crosslinker to prevent undesirable diluting disassembly, but proved to be a result of highly self-organization rather than random arrangement of the hybrid macromolecule upon the natural assembly operation.

References

[1] Gamys CG, Beyou E, Bourgeat-Lami E. Journal of Polymer Science: Part A: Polymer Chemistry **2010**; 48: 784–93.

[2] Mu¨llner M, Schallon A, Walther A, Freitag R, Mu¨llner AHE. Biomacromolecules **2010**; 11: 390–6.

[3] Qi XY, Xue C, Huang X, Huang Y, Zhou XZ, Li H, et al. Adv. Funct. Mater. **2010**; 20: 43–9.

[4] Murakami K, Aoki H, Nakamura S, Nakamura SI, Takikawa M, Hanzawa M, et al.Biomaterials **2010**; 31: 83-90.

[5] Wang GH, Zhang LM. J. Phys. Chem. B **2006**; 110: 24864-8.

[6] Tripathi BP, Shahi VK. J. Phys. Chem. B **2008**; 112 (49): 15678–90.

[7] Guo XH, Zheng D, Hu N. J.Phys. Chem. B **2008**; *112* (48): 15513–20.

[8] Liu KH, Chen SY, Liu DM, Liu TY. Macromolecules **2008**; 41: 6511-6.

[9] Fu L, Sa´ Ferreira RA, Silva NJO, Carlos LD. Chem. Mater. **2004**; 16*:* 1507-16.

[10] Bermudez VZ, Carlos LD, Alca´cer L. Chem. Mater. **1999**; 11: 569-80.

[11] Mahapatro A, Johnson DM, Patel DN, Feldman MD, Ayon AA, Agrawal CM. Langmuir **2006**; 22: 901-5.

[12] Yan E, Ding Y, Chen CJ, Li R, Hu Y, Jiang X. Chem. Commun. **2009**; 12: 2718–20.

[13] Franville AC, Mahiou R, Zambon D, Cousseins JC. Solid State Sciences **2001**; 3: 211–22.

[14] Goncüalves MC, Bermudez VZ, Sa´ Ferreira RA, Carlos LD, Ostrovskii D, Rocha J. Chem. Mater. **2004**; 16: 2530-43.

[15] Silva SS, Ferreira RAS, Fu L, Carlos LD, Mano JF, Reisab RL, et al. J. Mater.

Chem. **2005**; 15: 3952–61.

[16] Carlos LD, Sa´ Ferreira RA, Orion I, Bermudez VZ, Rocha J. J. Lumin. **2000**; 87: 702-5.

[17] Lin CL, Shih CL, Chau LK. Anal. Chem. **2007**; 79 : 3757-63.

[18] Yavuz MS, Cheng YY, Chen JY, Cobley CM, Zhang Q, Rycenga M, et al. Nature **2009**; 8: 935-9.

[19] Liu Li, Xu Xian, Guo S, Han W. Carbohydrate Polymers **2009**; 75: 401–7.

[20] Zhu A, Chan-Park MB, Dai S, Li L. Colloids Surf. B **2005**; 43: 143–9.

[21] Wang Y, Liu L, Weng J, Zhang Q. Carbohydr. Polym. **2007**; 69: 597–606.

[22] Li G, Zhuang Y, Mu Q, Wang M, Fang Y. Carbohydr. Polym. **2008**; 72: 60–6.

[23] Wilhelm M, Zhao C, Wang Y, Xu R, Winnik MA, Mura J. Macromolecules **1991**; 24: 1033–40.

[24] Amiji MM. Carbohydr. Polym. **1995**; 26: 211–3.

[25] Lee KY, Jo WH. Langmuir **1998**; 14: 2329–32.

[26] Hu FQ, Liu LN, Du YZ, Yuan H. Biomaterials **2009**; 30: 6955-63.

[27] Sun ZC, Bai F, Wu HM, Schmitt SK, Boye DM, Fan HY. J. Amer. Chem. Soc. **2009**; 131: 13594–5.

[28] Wen J, Wilkes GL. Chem. Mater. **1996**; 8: 1667-81.

[29] Ritger PL, Peppas NA. J. Controlled Release **1987**; 5: 37-42.

[30] Fini A, Orienti I. *Am. J. Drug Delivery* **2003**; *1*: 43–59.

[31] Lee M, Nah JW, Kwon Y, Koh JJ, Lo KS, Kim SW. *Pharm. Res.* **2001**; *18*: 427–31.

[32] Muzzarelli RAA, Muzzarelli C. *Adv. Polym. Sci.* **2005**; *186*: 151–209.

[33] Zhao AJ, Yuan XB, Chang J. *Polym. Bull.* **2004**; *4*: 59–63.

[34] Chae SY, Son S, Lee M, Jang MK, Nah JW. *J. Controlled Release* **2005**; *109*:330–44.

[35] Suia W, Songa G, Chenb G, Xuc G. *Colloids Surf., A* **2005**; *256*: 29–33.

[36] Letchford K, Burt H. Eur. J. Pharm. Biopharm. **2007**; 65: 259–69.

[37] Chiappetta DA, Sosnik A. Eur. J. Pharm. Biopharm. **2007**;66: 303–17.

[38] Sezgin Z, Yu ksel N, Baykara T, Eur. J. Pharm. Biopharm. **2006**; 64: 261–8.

[39] Zuccari G, Carosio R, Fini A, Montaldo PG, Orienti I. J. Control. Release **2005**;103: 369–80.

[40] Liu P, Wang BC, Li J, Qiao WL. Med. Hypotheses **2008**; 71: 379–81.

[41] Young C, Ozols RF, Myers CE. *New Engl. J. Med.* **1981**;*30:* 139–153.

[42] Takahashi T, Yamada Y, Kataoka K, Nagasaki Y. Journal of Controlled Release **2005**; 107: 408-16.

[43] Paul G, Heimink J, Koller H. Chem. Mater. **2008**; 20: 5083-9.

[44] Azzam T, Domb AJ. Current Drug Delivery **2004**; 1: 165-193.

[45] Garnett MC. Critical Review in Therapeutic Drug Carrier Systems **2004**; 16: 147-207.

[46] Rolland A. Harwood, Amsterdam **1999**.

[47] Kneuer C, Sameti M, Bakowsky U, Schiestel T, Schirra H, Schmidt H, Lehr CS. Bioconjugate chemistry **2000**; 11: 926-32.

[48] Kneuer C, Sameti M, Haltner EG, Schiestel T, Schirra H, Schmidt H, Lehr CS.International Journal of Pharmaceutical **2000**; 196: 257-261.

[49] Sanhu KK, McIntosh CM, Simard JM, Smith SW, Rotello VM. Bioconjugate Chemistry **2002**; 13: 3-6.

[50] Kubo T, Sugita T, Shimose S, Nitta Y, Ikuta Y, Murakami T. International Journal of Oncology **2001**; 18: 121-5.

[51] Berry CC, Curtis ASG. Journal of Physics D: Applied Physics **2003**; 36: R198-206.

[52] Zhu SG, Xiang JJ, Li XL, Shen SR, Lu HB, Zhou J, et al. Biotechnology of Applied Biochemistry **2004**; 39: 179-187.

[53] Gupta AK, Curtis ASG. Biomaterials **2004**; 25: 3029-40.

無研發成果推廣資料

98 年度專題研究計畫研究成果彙整表

計畫主持人：劉典謨	計畫編號：98-2113-M-009-004-
計畫名稱：以無機分子改質雙性機丁聚糖之自組裝混成複合材料及其生醫特性之研究	

成果項目			量化			單位	備註（質化說明：如數個計畫共同成果、成果列為該期刊之封面故事...等）
			實際已達成數（被接受或已發表）	預期總達成數(含實際已達成數)	本計畫實際貢獻百分比		
國內	論文著作	期刊論文	1	1	100%	篇	
		研究報告/技術報告	0	0	100%		
		研討會論文	0	0	100%		
		專書	0	0	100%		
	專利	申請中件數	2	2	100%	件	
		已獲得件數	0	0	100%		
	技術移轉	件數	0	0	100%	件	
		權利金	0	0	100%	千元	
	參與計畫人力（本國籍）	碩士生	2	2	100%	人次	
		博士生	0	0	100%		
		博士後研究員	0	0	100%		
		專任助理	0	0	100%		
國外	論文著作	期刊論文	0	0	100%	篇	
		研究報告/技術報告	0	0	100%		
		研討會論文	0	0	100%		
		專書	0	0	100%	章/本	
	專利	申請中件數	0	0	100%	件	
		已獲得件數	0	0	100%		
	技術移轉	件數	0	0	100%	件	
		權利金	0	0	100%	千元	
	參與計畫人力（外國籍）	碩士生	0	0	100%	人次	
		博士生	0	0	100%		
		博士後研究員	0	0	100%		
		專任助理	0	0	100%		

其他成果 (無法以量化表達之成果如辦理學術活動、獲得獎項、重要國際合作、研究成果國際影響力及其他協助產業技術發展之具體效益事項等，請以文字敘述填列。)	無

	成果項目	量化	名稱或內容性質簡述
科教處計畫加填項目	測驗工具(含質性與量性)	0	
	課程/模組	0	
	電腦及網路系統或工具	0	
	教材	0	
	舉辦之活動/競賽	0	
	研討會/工作坊	0	
	電子報、網站	0	
	計畫成果推廣之參與（閱聽）人數	0	

國科會補助專題研究計畫成果報告自評表

請就研究內容與原計畫相符程度、達成預期目標情況、研究成果之學術或應用價值（簡要敘述成果所代表之意義、價值、影響或進一步發展之可能性）、是否適合在學術期刊發表或申請專利、主要發現或其他有關價值等，作一綜合評估。

1. 請就研究內容與原計畫相符程度、達成預期目標情況作一綜合評估

■達成目標

□未達成目標（請說明，以 100 字為限）

□實驗失敗

□因故實驗中斷

□其他原因

說明：

2. 研究成果在學術期刊發表或申請專利等情形：

論文：■已發表 □未發表之文稿 □撰寫中 □無

專利：□已獲得 ■申請中 □無

技轉：□已技轉 □洽談中 ■無

其他：(以 100 字為限)

3. 請依學術成就、技術創新、社會影響等方面，評估研究成果之學術或應用價值（簡要敘述成果所代表之意義、價值、影響或進一步發展之可能性）(以 500 字為限)

有機-無機混成分子可藉由其自組裝的特性，提供一簡易藥物包覆途徑，其藥物包覆率高，二氧化矽層在此混成奈米微粒中，扮演著物理屏障的角色，可以減少包覆之內容物隨著高分子在水溶液中膨潤現象的產生而擴散溢出，因而達到藥物緩慢釋放之效果。細胞生物應用方面，此載體生物相容性高，對於正常細胞之毒殺性極低，且能夠快速的被細胞藉由胞吞作用攝入於細胞內，顯示此新型的有機-無機混成分子能有效把包覆於其中之活性藥物帶入細胞內並達到治療之效用。

計畫成果已達預期目標，開發一具生物相容性良好之新型有機-無機混成分子，未來可用於美妝保養、食品、口服劑型、抗癌藥物載體等多方面生醫之應用。美妝應用上，傳統保養品由於分子顆粒過大，使有效成分無法進入皮膚深層，藉由此載體包覆可以攜帶有效成分並釋放於皮膚底層，發揮保養之效果。於口服應用方面，服用藥物或是保健食品易受到人體內消化道酵素及酸性環境所破壞而降低藥物效果，將食入藥物包裹於其中，可免受藥物服用過程中外在環境的破壞以提高療效。此載體具有高載藥量、毒性極低，因此在藥物、食品、美妝品皆具潛力之發展。